INSTITUT CATALÀ DE CIÈNCIES DEL CLIMA

Institut Català de Ciències del Clima

C/ Doctor Trueta, 203
Barcelona, 08005
Phone: +34 93 309 7600
Web: www.ic3.cat

002

SEASONAL PREDICTION WITH EC-EARTH 3: IMPACT OF RESOLUTION AND INIITALISATION OF SEA ICE AND LAND SURFACE

O. Bellprat, D. Macias-Gómez, C. Prodhomme, V. Guemas and F. Doblas-Reyes

Climate Forecasting Unit
Institut Català de Ciències del Clima

03 September 2015

TECHNICAL MEMORANDUM

Series : CFU Technical Memoranda

A full list of CFU Publications can be found on our website under:

http://ic3cfu.wikispot.org

Fundació Institut Català de Ciències del Clima (IC3)
C/ Doctor Trueta, 203 | 08005 Barcelona

1. Introduction

Climate prediction is a rapidly emerging field that aims predicting the natural climate variability and climate change in the intraseasonal-to-interannual timescales using state-of-the-art climate models. The predictions offer the opportunity to provide information about the state of the Earth's system in the scales between numerical weather prediction and projections of climate change needed by many public sectors such as agriculture, energy production and human health (Challinor et al., 2005, García-Morales et al., 2007, Thomson et al., 2006).

A key aspect in climate forecasting, commonly also embraced under the term seasonal-to-decadal forecasting, is the verification of the systems to evaluate the trustworthiness of the predictions. Predictions that do not prove to be skillful are of no use and can even cause wrong decisions leading to socio-economic impacts (Weissheimer and Palmer, 2014). The evaluation of the systems is performed under a process termed *forecast quality assessment* which relies on retrospective predictions of the past climate using model hindcasts. The systems predict in this process the past climate for which observations are already available. Using these hindcasts the average skill of the systems can be computed. The hindcasts are also a necessary step to understand whether developments in a climate forecast system lead to an improvement in the predictions (Doblas-Reyes et al., 2013).

Two examples for improving the systems to which research is currently devoted is increase in the horizontal resolution of the climate models (Jung et al., 2012) and the initialisation of land surface (Prodhomme et al., 2015) and sea-ice conditions (Guemas et al., 2014). Using the EC-Earth atmosphere-ocean coupled climate model (Hazeleger et al. 2012) these two aspects are being evaluated using a new set of model hindcasts performed under the project "VERification of high-resolution climate forecasts on Intraseasonal-to-interannual Timescales with Advanced Satellite datasets of the Climate Change Initiative" (VERITAS-CCI). The new hindcasts will allow to evaluate the prospects of horizontal resolution and initialisation techniques using new observational records that have been independent in from previous model evaluations and that allow to asses the importance of observational uncertainty in the forecast quality assessment process.

This technical report provides the description of the model hindcasts that have been conducted and shows first insights from the experiments and the consideration of observational uncertainty.

2. Hindcasts and observations

The importance of model initialization for the land-surface and sea ice, as well as the prospects from an increasing model resolution is studied using a matrix of six sets of seasonal hindcasts described in Table 1 (for the realistic initialisation hindcast two hindcasts are carried out for each land-surface and sea-ice experiment).

Resolution | *Initialisation*	Realistic Init	Clim. land-surface init	Clim. sea-ice init
Low resolution (T255ORCA1)	**$x_{1,2}$**	**x**	**x**
High-resolution (T511ORCA025)	**x**	**x**	

Table 1: EC-Earth hindcasts to study effects of horizontal resolution and initialisation of land surface and sea ice. Two hindcasts for the hindcast of the realistic initialisation were performed since the sea-ice experiment were conducted with EC-Earth v2.3

The model resolution is classified into two setups, low resolution and high resolution. The low resolution uses a spectral truncation of the atmospheric model (IFS) at T255 (approx. 80 km globally) and grid resolution of the ocean model (ORCA) of 1° globally (approximately 100 km). The high resolution uses a truncation of T511 (approx. 40 km globally) and 0.25° (approx. 25 km globally) for the ocean. The initialisation of the land surface and sea ice is tested using realistic initialisation with observationally constrained conditions for the land-surface and sea ice and climatological conditions for the land-surface and sea-ice. The hindcasts are performed with the latest EC-Earth version 3.1 while the sea-ice initialisation hindcasts were performed with a former version, EC-Earth 2.3.

The hindcasts are initialized with the ocean re-analysis GLORYS2v1 (Ferry et al., 2010), ERA-Interim for the atmosphere (Dee et al., 2011), ERA-Land (Balsamo et al., 2015) for the land-surface and sea-ice initial conditions from (Guemas et al., 2014). For the hindcasts of the climatological conditions the climatology of the land-surface and sea-ice conditions are computed for a window of 10 days around the starting month of the predictions. The starting months of the predictions are May and November from which four and six months (only for the sea-ice experiments) integrations are computed for each year in 1993 to 2009. Each prediction consists of ten ensembles members generated using singular vectors to sample efficiently the natural variability. The total number of simulations corresponds therefore to 340 simulations of four months for each hindcast.

The hindcasts are evaluated in this technical report for sea-surface temperatures (SSTs), two-metre air temperature (T2M) and sea-ice extent (SIE). Several sets of observations are considered for the estimation of the SST prediction skill, ESA CCI, HadISST (Rayner et al., 2003), ERA-Interim (Dee et al., 2011) and ERSST (Smith and Reynolds, 2003), as part of an assessment of the observational uncertainty. For T2M European temperatures predictions are analyzed for the experiments of the land-surface initialization for which the E-OBS (v.10) (Haylock et al., 2008). For the sea-ice experiments we analyze sea-ice extent from ESA CCI over the Arctic sea regions.

For the verification of SSTs we further consider the observational error estimates provided by ESA CCI. The observational error is provided at a daily scale whereas in climate predictions typically monthly averages are verified. The CCI SST project team developed an SST interpolation tool to re-estimate observational uncertainty at different spatio-temporal scales yet the application has not been made ready yet for distribution. Scaling the observational error estimates for larger averages using the root of the number of data points included in an average as a common scaling of error apparently would underestimate the observational uncertainty (C. Merchant, personal communication) and hence in this application the same error estimates as at the daily scales are used. This is clearly an overestimation of the observational error and the correct estimates using the SST processing tool will be conducted once the product is available. Using the current error estimates, observational members are generated using a Gaussian distribution with zero mean and standard deviation of the error estimates, neglecting error-covariates.

3. First insights and importance of observational uncertainty

3.1 Low versus high model resolution

Preliminary insights comparing the different hindcasts illustrated here show promising results including observations provided by ESA CCI. Figure 1 shows an analysis on the prediction skill of the El Niño Southern Oscillation (ENSO). A common measure to verify ENSO prediction skill is the temporal correlation of the ensemble mean of the prediction (10 members) for each forecast month after the initialization of the prediction for the Niño3.4 index. Panel (a) shows the correlation for summer months, varying from initially 0.9-1 to 0.7-0.8 in August. There are high correlation values compared to other seasonal prediction systems. The figure shows that depending on which observational reference dataset considered the prediction skill varies considerably yet the pattern remains surprisingly robust (correlations are usually higher with ESA CCI and lower with ERSST as reference).

The comparison to the low-resolution hindcasts shown in panel (b) reveals that the increase in horizontal resolution improves the ENSO prediction skill significantly and most predominantly as the forecast time increases. The correlation increase is of the order of 0.1, which is given the already high values of correlation a large improvement, statistically significant at the 1% significance level. Understanding this improvement will be the objective of future analysis.

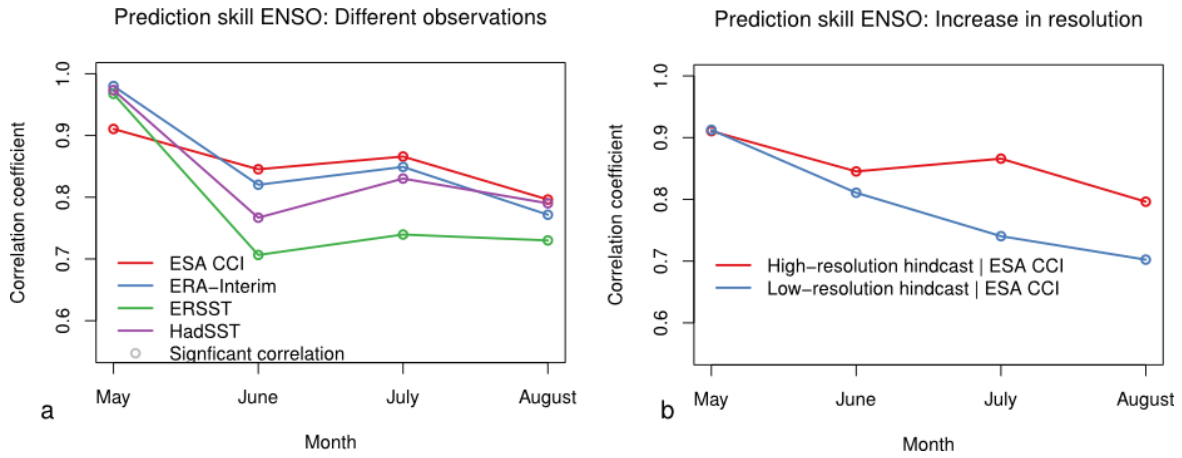

Figure 1: (a) Temporal correlation of Niño 3.4 SSTs over the hindcast period (1993-2009) for each forecast month of the high-resolution hindcasts using realistic initial conditions for predictions started in summer. The correlation coefficients are shown for four different observational datasets and circles denote correlations that are significant at the 5% significance level. (b) Comparison of changes in the horizontal resolution using the high-resolution (red) and low-resolution (blue) hindcast for the same correlation analysis using only the ESA CCI observations as reference. Difference in the correlation are significant at the 1% confidence level.

3.2 Land-surface initialisation

The effect of the land-surface initialisation is illustrated in figure 2, which shows the skill of summer air temperatures over Europe as numerous studies have highlighted the importance of land-surface coupling in this region (Seneviratne et al., 2010). The figure shows, as in figure 1, the temporal correlation for all land points over Europe. Panel (a) shows the correlation coefficient with climatological land-surface conditions, which show positive skill over central Europe (stippling indicates significant correlation), but low or even negative correlation values over other Scandinavia, Eastern and Southern Europe. The hindcast with realistic land-surface initialisations greatly improves the summer prediction skill showing that for large fraction of Europe a significant skill in seasonal summer prediction emerges. The difference of the two hindcasts is shown in panel (c) which highlights that land-surface conditions particularly improve the predictions for Southern and Eastern Europe but also for Scandinavia consistent with former studies on land-surface coupling over Europe (Bellprat et al., 2015). However, the skill over the British Isles deteriorates. Further analysis on the evolution of soil-moisture using the ESA soil moisture datasets will follow.

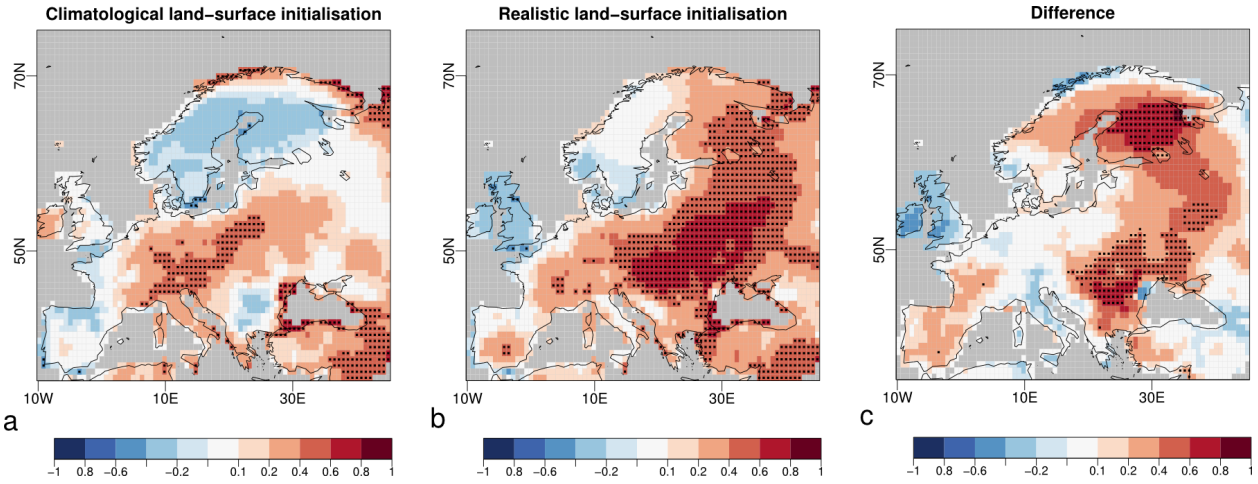

Figure 2: Temporal correlation over land points for summer (JJA) averages between hindcast with (a) climatological land-surface initialisation and (b) realistic land-surface initialisation with the E-OBS 2m temperature observations. Panel (c) shows the difference of the two hindcasts whereas the stippled points show significant correlation or significant difference in correlation both at the 5% significance level. The hindcast are run at high horizontal resolution.

3.3. Sea-ice initialisation

The first analysis on the sea-ice initialisation experiments is based on Arctic sea ice cover by computing the monthly extent (Notz et al., 2014). We compare for this purpose in figure 3 firstly two different datasets, ESA CCI and NSIDC, for the annual minimum sea-ice extent in September (which is when the minimum extent is typically recorded) during the period (1993-2010). The inter-annual variability of the datasets is very similar, yet the ESA CCI gives about 1 Mio.m² more ice extent than NSIDC. A possible explanation of this difference may come from the much higher resolution of ESA CCI (0.25°), which might result in an increased total sea area by resolving the Canadian archipelago more accurately. However, a notable difference between the datasets in terms of variability is the year 2010, which is the lowest sea-ice extent in ESA CCI but not in NSIDC (for which the minimum is recorded in 2007).

The difference in the observational datasets appears also in the skill of the hindcasts for the summer sea-ice extent. The temporal correlation of the hindcast with realistic sea-ice initialisation is systematically larger with the ESA CCI dataset. This difference due to

the dataset is not obvious because, and equally in figure 1, the correlation is not a measure of distance. The systematic better agreement between the model and the observations when using the CCI data has therefore implications on the covariances and the level of noise in the observations. The hindcasts show reasonable prediction skill with both observational datasets, which suggest that a comparison to a persistence forecast is needed to demonstrate whether true dynamical skill emerges. The difference in the climatological and realistic initialization is striking because no skill appears in the climatological forecast in the first month but later skill emerges. Further analysis is though required to understand this behavior properly.

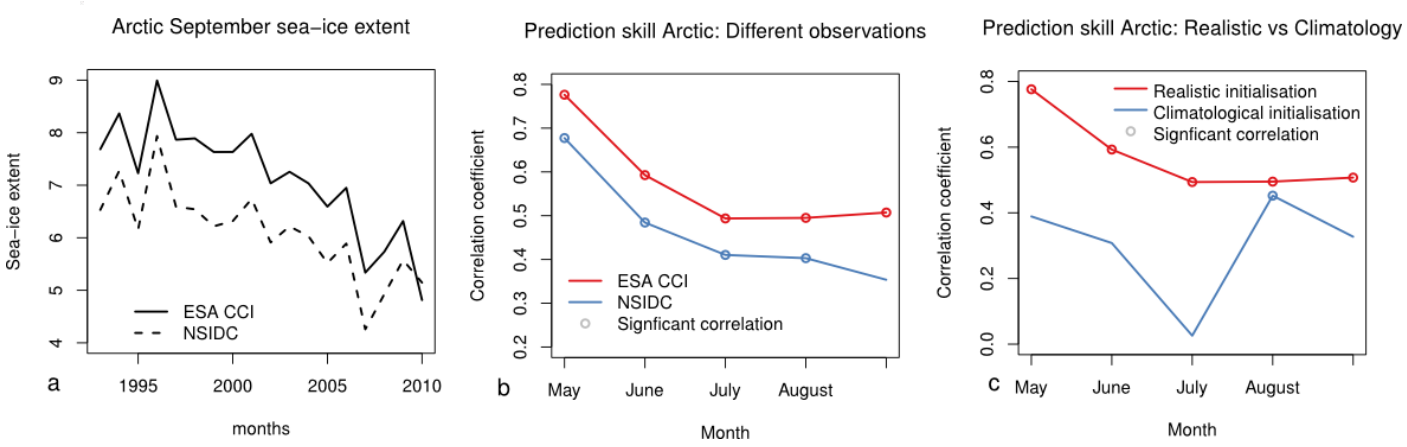

Figure 3: Analysis of Arctic sea-ice extent. (a) Comparison of two observational datasets ESA CCI and NSIDC for September (Arctic sea-ice annual minimum) extent (b) Correlation of predictions starting in May for the two observational datasets with significant correlation in circled points (5% significance level). (c) Correlation of realistic (red) in comparison to climatological (blue) initialisation using ESA CCI as reference.

3.4 Importance of observational uncertainty in verification

Observational uncertainty can play an important role in the evaluation of climate models (Bellprat et al., 2012) and can alter a verification statement as illustrated in figure 1 using different observational datasets. Although its relevance is not questioned, currently very little efforts are devoted to include observational uncertainty estimates in forecast verification and methodological grounds remain sparsely explored. The ESA CCI datasets have placed a major effort in deriving robust observational uncertainty

estimates that are here placed in the context of forecast verification by comparing the observational uncertainty to other sources of uncertainty in climate forecasting.

The verification of climate forecast systems is subject to two major sources of uncertainty. The first source arises from the fact that hindcasts of the past climate can only be performed for a limited period, commonly constrained by the fact that robust initial conditions for the ocean are only available from the late 20th century. Typical hindcasts periods range therefore from 15 to 30 years, an aspect that introduces a major source of uncertainty in the verification statistics. This uncertainty is labelled here as the number of start dates uncertainty. Another source of uncertainty is related to the ensemble size in each predictions. For some processes a high ensemble size is required to robustly sample the natural variability, but for computational constraints often only about 10 ensemble members can be afforded. We refer here to this source as the member uncertainty in verification.

Figure 4 shows a comparison of the relative contribution of each source of uncertainty. The different sources are compared by bootstrapping the root mean square (RMS) deviation from the Niño3.4 SSTs (ESA CCI) for the different uncertainties individually using the low-resolution hindcast. The resampling is performed without blocks by replacing the sample of members, start dates or observational members by a randomized sample with replacement. The resulting variances of RMS for each source of uncertainty are consequently summed to form a total variance in order to display what the relative contribution from each source is. The figure shows that for the verification of ENSO the observational uncertainty is crucial during the course of the forecast accounting to about 40% of the uncertainty, yet this estimate is likely to be too large given the shortcomings of data described in the previous section. The largest source of uncertainty stems from the number of start dates, which is given the short periods of the analysed hindcasts (17 years) to be expected. The uncertainty arising from a limited number of members is almost negligible in this example. This is possibly a result of the RMS being computed from an ensemble average and that for the Niño3.4 region the spread of the members is relatively small given the high predictability of the variable in this region.

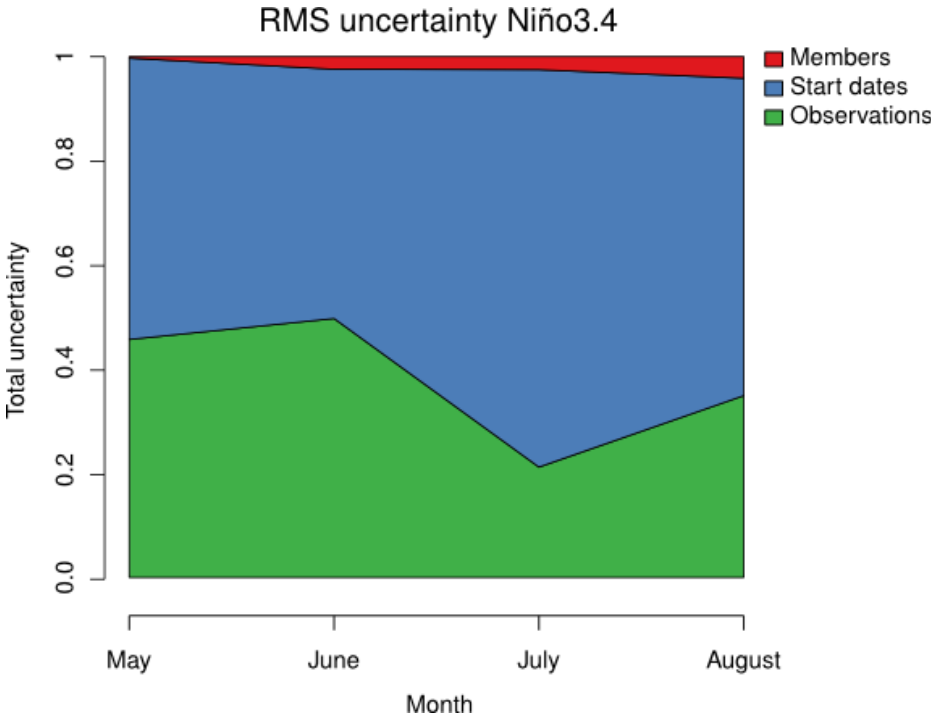

Figure 4: Uncertainty sources in terms of root mean square (RMS) deviations of SST over the Niño3.4 region for predictions starting in May. The sources of uncertainty are sampled by bootstrapping the RMS individually for each uncertainty source and adding the variances of the sources to a total uncertainty, similarly as in Hawkins and Sutton (2012). Three sources of uncertainty are considered: ensemble size, the number of start dates of the hindcasts and the observational uncertainty of the ESA CCI SST.

4. Conclusions and outlook

A new set of climate hindcasts using the EC-Earth climate forecast system have been carried out under the ESA Living Planet Fellowship project VERITAS-CCI. They have been completed successfully and preliminary results are described here. The aim of the hindcasts is to study the effect of increasing horizontal resolution and the initialisation of the land-surface and sea-ice to improve forecast quality. A first analysis of the hindcasts shows promising results that require, however, in-depth understanding at the process level to reveal promising premises for research. The analysis of the forecast skill has been conducted with the new ESA CCI datasets but also with other datasets to explore the observational uncertainty. The uncertainty that arises is large and requires more attention from the climate prediction community. Interestingly the observational uncertainty is surprisingly systematic in the sense that the e.g. the ESA CCI datasets provide the highest correlation scores for the model under consideration. The genuine aspect of correlation is that it increases when noise is reduced, in either model or observations, which is well known in the sense that increasing the forecast ensemble size increases the correlation (Scaife et al., 2014). Hence while the higher correlation might arise from a higher covariance of the variability in both model and observations it might tell us as well something about the instrumental noise level in the observations. This hypothesis needs though to be further analysed but shows a promising perspective on the importance of understanding observational uncertainty and support decisions about which observational datasets are preferable for verification. A more robust analysis will require multiple models hindcast.

References

Balsamo, G., et al (2015) ERA-Interim/Land: a global land surface reanalysis data set, Hydrol. Earth Syst. Sci., 19, 389-407, doi:10.5194/hess-19-389-2015 2015.

Bellprat, O., Kotlarski, S., Lüthi, D., and Schär, C. (2012a). Exploring Perturbed Physics Ensembles in a Regional Climate Model. Journal of Climate, 25(13), 4582–4599.

Bellprat, O., Kotlarski, S., Lüthi, D., R. De Elía, A. Frigon, R. Laprise and C. Schär (2015). Objective calibration of regional climate models: Application over Europe and North America. Journal of Climate, *submitted*

Challinor, A., Slingo, J., Wheeler, T., and Doblas-Reyes, F. (2005). Probabilistic simulations of crop yield over western India using the DEMETER seasonal hindcast ensembles. Tellus A, 57(3).

Dee, D. P., Uppala, S. M., Simmons, A. J., Berrisford, P., Poli, P., Kobayashi, S., Andrae, U., Balmaseda, M. A.,.Balsamo, G., Bauer, P., Bechtold, P., Beljaars, A. C. M., van de Berg, L., Bidlot, J., Bormann, N., Delsol, C., Dragani, R., Fuentes, M., Geer, A J., Haimberger, L., Healy, S. B., Hersbach, H., Holm, E V., Isaksen, L., Kallberg, P., Koehler, M., Matricardi, M., McNally, A. P., Monge-Sanz, B. M., Morcrette, J. J., Park, B. K., Peubey, C., de Rosnay, P., Tavolato, C., Thepaut, J. N., Vitart, F. (2011). The ERA-Interim reanalysis: configuration and performance of the data assimilation system. Quarterly Journal of the Royal Meteorological Society, 137(656), 553–597.

Doblas-Reyes, F. J., García-Serrano, J., Lienert, F., Biescas, A. P., & Rodrigues, L. R. L. (2013). Seasonal climate predictability and forecasting: Status and prospects. Wiley Interdisciplinary Reviews: Climate Change, 4(4), 245–268.

Ferry, N., L. Parent, G. Garric, B. Barnier, N. C. Jourdain and the Mercator Ocean team(2010). Mercator Global Eddy Permitting Ocean Reanalysis GLORYS1v1: Description and Results. *Mercator Ocean Quarterly Newsletter*, 36, 15-27.

García-Morales, M. B., & Dubus, L. (2007). Forecasting precipitation for hydroelectric power management : how to exploit GCM's seasonal ensemble forecasts, 1705, 1691–1705.

Guemas, V., Doblas-Reyes, F., Mogensen, K., Keeley, S., and Tang, Y. (2014). Ensemble of sea ice initial conditions for interannual climate predictions. Climate Dynamics, 1–17.

doi:10.1007/s00382-014-2095-7

Haylock, M.R., N. Hofstra, A.M.G. Klein Tank, E.J. Klok, P.D. Jones and M. New. 2008: A European daily high-resolution gridded dataset of surface temperature and precipitation. J. Geophys. Res (Atmospheres), **113**, D20119

Hazeleger, W., Severijns, C., Semmler, T., Ştefănescu, S., Yang, S., Wang, X., Wyser, K. Dutra, E., Baldasano, J. M., Bintanja, R., Bougeault, P., Caballero, R., Ekman, A. M. L. Christensen, J.H., van den Hurk, B., Jimenez, P., Jones, C., Kållberg, P., Koenigk, T., McGrath, R. Miranda, P. Van Noije, T., Palmer, T. Parodi, J., Schmith, T., Selten, F., Storelvmo, T., Sterl, A., Tapamo, H. Vancoppenolle, M., Viterbo, P., and Willén, U. (2010). EC-Earth: A Seamless Earth-System Prediction Approach in Action. Bulletin of the American Meteorological Society, 91(10), 1357–1363.

Jung, T., Miller, M. J., Palmer, T. N., Towers, P., Wedi, N., Achuthavarier, D., and Hodges, K. I. (2012). High-Resolution Global Climate Simulations with the ECMWF Model in Project Athena: Experimental Design, Model Climate, and Seasonal Forecast Skill. Journal of Climate, 25(9), 3155–3172.

Rayner, N. A., D. E. Parker, E. B. Horton, C. K. Folland, L. V. Alexander, D. P. Rowell, E. C. Kent, and A. Kaplan (2003), Global analyses of sea surface temperature, sea ice, and night marine air temperature since the late nineteenth century, *J. Geophys. Res.*, 108(D14), 4407.

Skillful Long Range Prediction of European and North American Winters by A. A. Scaife*, A. Arribas, E. Blockley, A. Brookshaw, R. T. Clark, N. Dunstone, R. Eade, D. Fereday, C. K. Folland, M. Gordon, L. Hermanson, J. R. Knight, D. J. Lea, C. MacLachlan, A. Maidens, M. Martin, A. K. Peterson, D. Smith, M. Vellinga, E. Wallace, J. Waters and A. Williams. *Geophysical Research Letters*. DOI: 10.1002/2014GL059637

Seneviratne, S. I., Corti, T., Davin, E. L., Hirschi, M., Jaeger, E. B., Lehner, I., Orlowsky, B., and Teuling, A. J. (2010). Investigating soil moisture-climate interactions in a changing climate: A review. Earth-Science Reviews, 99(3-4), 125–161.

Smith, T.M., and R.W. Reynolds, 2003: Extended Reconstruction of Global Sea Surface Temperatures Based on COADS Data (1854-1997). *J. Climate*, 16, 1495-1510.

Weisheimer A. and Palmer T. N. (2014). On the reliability of seasonal climate forecasts. J. R. Soc. Interface, 20131162. doi:10.1098/rsif.2013.1162 1742-5662